

Perturbation Method for Elementary Excitation of Liquid ${}^4\text{He}$ *

FELIX J. LEE (李俊弘)

*Physics Department, National Tsing Hua University
Hsinchu, Taiwan, Republic of China*

and

DEOK KEO LEE

Oak Ridge National Laboratory, Oak Ridge, Tennessee 37830, USA

(Received 11 March 1977)

Elementary excitation energy of liquid ${}^4\text{He}$ has been studied by using the Brillouin-Wigner perturbation theory in conjunction with the correlated basis functions. The leading correction to the convolution approximation for the three-particle distribution function, and the two-ring diagrams have been included. In the numerical calculation, the optimum liquid structure functions obtained by Campbell-Feenberg and by Pokrant are employed. In the Bijl-Dingle-Jastrow representation, Campbell-Feenberg's liquid structure function in the hypernetted-Chain approximation generates the best excitation spectrum in agreement with experiments. However, in the exact ground-state representation, all of the optimum forms considered yield poor agreements more or less. This indicates that the optimized BDJ-type of the liquid structure functions are still far from being considered as exact.

I. INTRODUCTION

In a previous paper⁽¹⁾, we have given rise to an encouraging agreement of the elementary excitation of liquid ${}^4\text{He}$ with experiments, based on the Bijl-Dingle-Jastrow representation. As mentioned there, the novel points include: i) the improvement to the convolution approximation (CA) for the three-particle distribution function $P^{(3)}$ (1, 2, 3) in evaluating the single-ring perturbation correction, ii) carrying out the Brillouin-Wigner (BW) energy series by incorporating all two-ring perturbations except diagrams containing zero-to-three/or three-to-zero phonon processes, iii) numerical calculations are done by using the optimum liquid structure function $S(k)$ obtained by Campbell and Feenberg (CF)⁽²⁾ in the hypernetted-Chain approximation.

In this paper, we first repeat the procedure of Ref. 1, by applying other values of $S(k)$ at hand, such as obtained by CF in the Percus-Yevick approximation and by Pokrant⁽³⁾ with bridge diagrams. Although these $S(k)$ yield better⁽²⁻⁴⁾ ground-state energy, results of the excitation spectrum show that $S(k)$ in the HNC approximation leads to the best agreements. This coincides with conclusions of many authors.

The criterion of disregarding diagrams with zero-to-three/or three-to-zero phonon processes is due to the numerical observation (except in small k region):

* Work supported partly by National Science Council of the Republic of China.

(1) D.K. Lee and F. J. Lee, Phys. Rev. **B11**, 4318 (1975).

(2) C.E. Campbell and E. Feenberg, Phys. Rev. 188, 396 (1969).

(3) M.A. Pokrant, Phys. Rev. A6, 1588 (1972).

(4) F. J. Lee and D. K. Lee, will be published.

$$|\langle \mathbf{k}, \mathbf{k}', \mathbf{k}'' | \delta H | 0 \rangle| \ll |\langle -\mathbf{k}', -\mathbf{k}'' | \delta H | \mathbf{k} \rangle| \quad (1)$$

in cases of $\mathbf{k} + \mathbf{k}' + \mathbf{k}'' = 0$, and $k = k' = k''$. This simplification is equivalent to surmise that the consideration of these diagrams can only suppress the first peak slightly, and contribute to the roton minimum and large k region negligibly. Now we are ready to confirm this by calculating through all two-ring diagrams containing single zero-to-three/or three-to-zero phonon process.

Also the elementary excitation has been derived by Jackson and Feenberg (JF)⁽⁵⁾ using the improved BW perturbation procedure. Under the CA expression for $P^{(3)}$, they evaluated the series with one-ring perturbation, and got improved agreement with experiment qualitatively. Following their procedure outlined, many authors⁽⁶⁻⁸⁾ extended the energy series to high-order corrections, including two-ring diagrams. Unfortunately, the series has only applied, so far, to the long wavelength limit. In this paper, we calculate the series for the elementary excitation by taking the leading correction to the CA for $P^{(3)}$ into account.

However, the JF method needs to use the exact $S(k)$ which is difficult even if possible to obtain accurately. By applying the optimum $S(k)$ in the JF formulism, results show poor agreement with experiments. The roton minimum is strongly cancelled by the third-order perturbation. This discrepancy may be interpreted that the optimum liquid structure functions are not good enough to be considered as exact. The exact $S(k)$ must be generated by the exact ground-state wavefunction.

For brevity we list only some basic formulas for the BDJ method in Sec. II, and for the JF method in Sec. III. As to detailed description and derivation, we refer to Refs. 1, 5, and 6. The numerical results of the excitation spectrum are given in Sec. IV, and a few including remarks are made in Sec. V.

II. OPTIMIZED BDJ METHOD

The system of interest consists of N bosons interacting in a box of volume Ω via a two-body potential $V(r)$. The Hamiltonian is given by

$$H = -\frac{\hbar^2}{2m} \sum_{i=1}^N \nabla_i^2 + \sum_{i < j} v(r_{ij}), \quad (2)$$

with the optimum BDJ-type wavefunction

$$\psi_0 = |0\rangle = \prod_{i < j} \exp \frac{1}{2} u(r_{ij}) / \left[\int \prod_{m < n} \exp u(r_{mn}) d\mathbf{r}_{1,2,\dots,N} \right]^{1/2}. \quad (3)$$

The n -particle distribution function

$$P^{(n)}(1, 2, \dots, n) = N(N-1) \dots (N-n+1) \int \psi_0^n d\mathbf{r}_{n+1, n+2, \dots, N}, \quad (4)$$

on the one hand, give the radial distribution and the liquid structure functions as

$$g(r_{12}) = \rho^{-2} P^{(2)}(1, 2), \quad (5)$$

$$S(k) = 1 + \rho \int [g(r) - g(\infty)] e^{i\mathbf{k}\cdot\mathbf{r}} d\mathbf{r}, \quad (6)$$

with the particle density $\rho = N/\Omega$, and on the other hand, allow the approximation

$$P^{(3)}(1, 2, 3) = P_c^{(3)}(1, 2, 3) + \delta P_c^{(3)}(1, 2, 3), \quad (7)$$

while the CA expression for $P_c^{(3)}$, and the leading correction $\delta P_c^{(3)}$ are derived explicitly in Ref. 1. The perturbation operator is defined by

$$\delta H = H - E_0 - \epsilon_0(k), \quad (8)$$

with the BDJ ground-state energy E_0 , and the Bijl-Feynman energy $\epsilon_0(k)$. Using the ordinary

(5) H. W. Jackson and E. Feenberg, Rev. Mod. Phys. 34, 686 (1962).

(6) D. K. Lee, Phys. Rev. 162, 134 (1967).

(7) F. J. Lee and D. K. Lee, Phys. Rev. A9, 1408 (1974).

(8) H. W. Lai, H. K. Sim, and C. W. Woo, Phys. Rev. A1, 1536 (1970).

perturbation theory, the diagrammatic representations including the dominant fourth order perturbations are plotted in Figs. 1 and 2, while Fig. 1 is reproduced from Ref. 1. Here we have dropped a lot of two-ring diagrams, such as shown in Fig. 3. Each diagram in Fig. 3 contains two small vertices: zero-to-three/ or three-to-zero, and one-to-three/ or three-to-one phonon processes. Consequently, the contribution of Fig. 3 is supposed to be smaller than that from Fig. 2. This

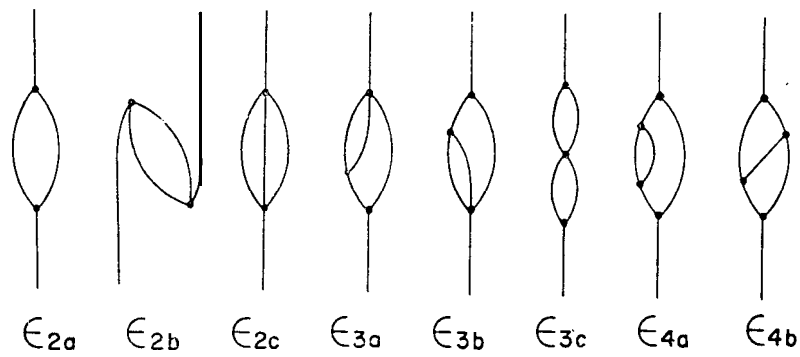


Fig. 1. Energy diagrams used in Ref. 1 to calculate Eq. (12).

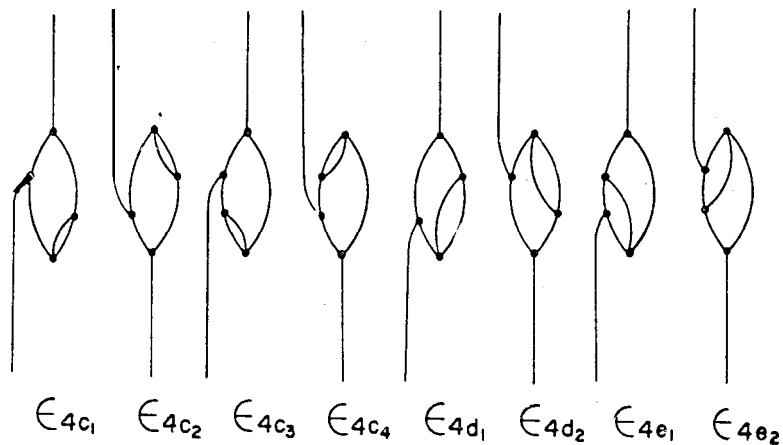


Fig. 2. Extra energy diagrams added at the present analysis to calculate $r(k)$ in the BDJ method.

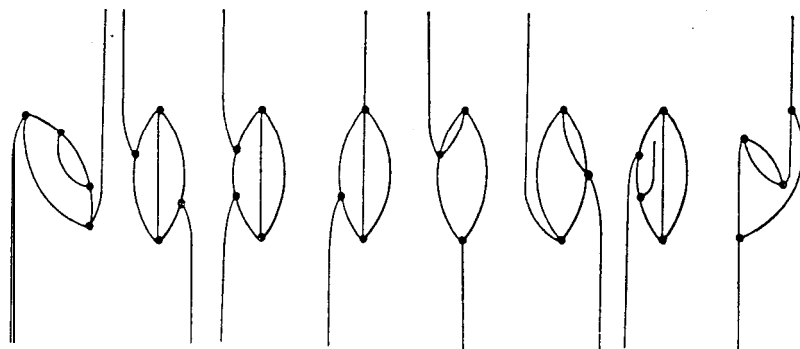


Fig. 3. Two-ring diagrams neglected in the calculation of $c(k)$.

simplification, of course, stands on the inequality of Eq. (1), and the numerical fact of $\epsilon_{3a}(k)$ and $\epsilon_{3b}(k)$ in Ref. 1.

The mathematical expressions of the additional diagrams in Fig. 2 are

$$\begin{aligned} \epsilon_{4c_1}(k) &= \epsilon_{4c_2}(k) = \epsilon_{4c_3}(k) = \epsilon_{4c_4}(k) = \frac{1}{2} \epsilon_{4c}(k) \\ &= \frac{\Omega^2}{2(2\pi)^6} \iint d\mathbf{k}' d\mathbf{k}_1 \frac{\langle \mathbf{k} | \delta H | \mathbf{j}-\mathbf{k}', -\mathbf{k}'' \rangle \langle -\mathbf{k}'' | \delta H | \mathbf{k}, \mathbf{k}' \rangle \langle -\mathbf{k}' | \delta H | \mathbf{k}_1, \mathbf{q} \rangle \langle \mathbf{k}', \mathbf{k}_1, \mathbf{q} | \delta H | 0 \rangle}{[\epsilon(k) - \epsilon_0(k') - \epsilon_0(k'')] [\epsilon(k) - \epsilon_0(k) - 2\epsilon_0(k')] [\epsilon(k) - \epsilon_0(k) - \epsilon_0(k') - \epsilon_0(k_1) - \epsilon_0(q)]}, \end{aligned} \quad (9)$$

$$\begin{aligned} \epsilon_{4d_1}(k) &= \epsilon_{4d_2}(k) = \frac{1}{2} \epsilon_{4d}(k) \\ &= \frac{\Omega^2}{2(2\pi)^6} \iint d\mathbf{k}' d\mathbf{k}_1 \frac{\langle \mathbf{k} | \delta H | -\mathbf{k}', -\mathbf{k}'' \rangle \langle -\mathbf{k}'' | \delta H | \mathbf{k}, \mathbf{k}' \rangle \langle -\mathbf{k}' | \delta H | \mathbf{k}_1, \mathbf{q} \rangle \langle \mathbf{k}', \mathbf{k}_1, \mathbf{q} | \delta H | 0 \rangle}{[\epsilon(k) - \epsilon_0(k') - \epsilon_0(k'')] [\epsilon(k) - \epsilon_0(k') - \epsilon_0(k_1) - \epsilon_0(q)] [\epsilon(k) - \epsilon_0(k) - \epsilon_0(k') - \epsilon_0(k_1) - \epsilon_0(q)]}, \end{aligned} \quad (10)$$

$$\begin{aligned} \epsilon_{4e_1}(k) &= \epsilon_{4e_2}(k) = \frac{1}{2} \epsilon_{4e}(k) \\ &= \frac{\Omega^2}{2(2\pi)^6} \iint d\mathbf{k}' d\mathbf{k}_1 \frac{\langle \mathbf{k} | \delta H | \mathbf{k}, \mathbf{q} \rangle \langle \mathbf{q} | \delta H | -\mathbf{k}'' \rangle \langle -\mathbf{k}'' | \delta H | \mathbf{k}, \mathbf{k}' \rangle \langle \mathbf{k}', \mathbf{k}_1, \mathbf{q} | \delta H | 0 \rangle}{[\epsilon(k) - \epsilon_0(p) - \epsilon_0(k_1)] [\epsilon(k) - \epsilon_0(k') - \epsilon_0(q) - \epsilon_0(k_1)] [\epsilon(k) - \epsilon_0(k) - \epsilon_0(k') - \epsilon_0(k_1) - \epsilon_0(q)]}, \end{aligned} \quad (11)$$

with $\mathbf{k} + \mathbf{k}' + \mathbf{k}'' = 0$, $\mathbf{q} + \mathbf{k}' + \mathbf{k}_1 = 0$, and $\mathbf{p} = \mathbf{k}' - \mathbf{k}_1$. In the accuracy of interest, the three-phonon process here can be replaced by the CA expression. The BW energy series associated with Fig. 1 is given by

$$\epsilon(k) = \epsilon_0(k) \epsilon_{2a}(k) + \epsilon_{2b}(k) + \epsilon_{2c}(k) + \epsilon_{3ab}(k) + \epsilon_{3c}(k) + \epsilon_{4a}(k) + \epsilon_{4b}(k), \quad (12)$$

described in Ref. 1. Hence, by adding perturbation diagrams shown in Fig. 2, our final perturbation series is read as

$$\begin{aligned} \epsilon(k) &= \epsilon_0(k) + \epsilon_{2a}(k) + \epsilon_{2b}(k) + \epsilon_{2c}(k) + \epsilon_{3ab}(k) + \epsilon_{3c}(k) \\ &\quad + \epsilon_{4a}(k) + \epsilon_{4b}(k) + \epsilon_{4c}(k) + \epsilon_{4d}(k) + \epsilon_{4e}(k). \end{aligned} \quad (13)$$

As well-known the use of the Rayleigh-Schrödinger perturbation formulas often encounters with zero denominator corresponding to real phonon splitting or coalescing process, whereas no such singularities happen to the BW formulas. This ensures that a final iteration value with physical meaning can be obtained, and result indeed represents the true solution.

III. JACKSON AND FEENBERG METHOD

The analysis of the elementary excitation by the JF method⁽⁵⁾ is similar to that of the BDJ calculation. It bases on the assumption that the exact ground-state properties are known instead of forms in the BDJ space, JF first evaluated the energy series to the second-order correction:

$$\epsilon(k) = \epsilon_0(k) + \epsilon_2^c(k), \quad (14)$$

with the superscript c denoting the use of the CA for $P^{(3)}$. Results show only qualitative agreement with experiment. They also surmised that the error introduced by neglecting higher-order corrections should be less than that associated with the approximate form for $P^{(3)}$. So far, this surmise has not been studied too much.

In a previous paper⁽⁷⁾, we found that the correction term $\delta P_2^{(3)}$ in the uniform limit could yield about 7.9% of the second-order correction energy in the long wavelength limit. This points out possibly that $P_2^{(3)}$ is only a rough approximation for the three-particle distribution function. Thus, even if the high-order corrections are neglected, a more accurate energy spectrum, at least, can be obtained by the use of the improved form of Eq. (7). The explicit expressions are

$$\epsilon(k) = \epsilon_0(k) + \epsilon_2^c(k) + \Delta \epsilon_2(k),$$

with

$$\Delta\epsilon(k) = \frac{\hbar^2}{2m} \frac{\epsilon_0(k)}{(2\pi)^3 \rho} \int d\mathbf{k}' \frac{\Delta(k, \mathbf{k}', k'')[(\mathbf{k} \cdot \mathbf{k}')S(k'') + (\mathbf{k} \cdot \mathbf{k}'')S(k') + k^2 S(k')S(k'')]}{\epsilon(k) - \epsilon_0(k') - \epsilon_0(k'')} + \frac{S(k)\epsilon_0^2(k)}{2(2\pi)^3 \rho} \int d\mathbf{k}' \frac{\Delta^2(k, \mathbf{k}', k'')S(k')S(k'')}{\epsilon(k) - \epsilon_0(k')\epsilon_0(k'')}, \quad (16)$$

$$\Delta(k, \mathbf{k}', \mathbf{k}'') = -(2\pi)^{-3} \rho^{-1} \int d\mathbf{q} F(\mathbf{q} + \mathbf{k}) F(\mathbf{q} - \mathbf{k}'). \quad (17)$$

Equation (17) is derived in Ref. 1.

As for the neglected higher-order corrections, the ordinary perturbation theory following the procedure by JF can be easily extended. In diagrammatic representation, the energy corrections through two-ring diagrams are reproduced^(7,9) in Fig. 4. Although these diagrams all shown up in Fig. 1. have the same mathematical expressions as counterparts in the BDJ space, the interpretations for the interaction matrix elements are completely different. The required matrix elements up to four-phonon processes are derived in detail in Ref. 6. Consequently, by taking account the two-ring perturbation, our BW energy series can be written as

$$\epsilon(k) = \epsilon_0(k) + \epsilon_2(k) + \epsilon_4(k) + \epsilon_{4a}(k) + \epsilon_{4b}(k), \quad (18)$$

with

$$\epsilon_2(k) = \epsilon_2^s(k) + \Delta\epsilon_2(k). \quad (19)$$

It is worth of noting here that matrix elements associated with two-ring diagrams in Eq. (18) are again evaluated with the CA expression for $P^{(9)}$. In the numerical computation, we actually use the improved BW perturbation procedure⁽⁹⁾ which rearranges Eq. (18) as

$$\epsilon(k) = \epsilon_0(k) + \frac{\epsilon_2^s(k)}{\epsilon_2(k) - \epsilon_3(k)} + \epsilon_{4a}(k) + \epsilon_{4b}(k), \quad (20)$$

in order to get lower upper bound values.

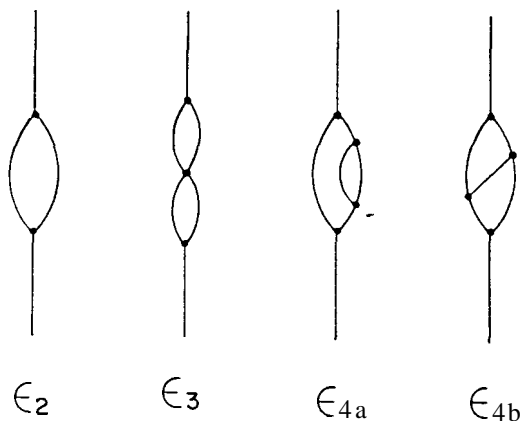


Fig. 4. Energy diagrams containing two-ring in the JF method.

IV. NUMERICAL EVALUATION

In carrying out the numerical iteration of Eqs. (12), (13) and (20), we keep in mind of accuracy that matrix elements are calculated using the CA expressions for two-ring diagrams and the improved form of Eq. (7) for single-ring. Since the final spectrum must be independent of the starting trial, iteration begins with the Cowley-Woods experimental measurement⁽¹⁰⁾. Moreover, in order to get the difference between two successive values less than 1% a fester, we make use of the mean as the

(9) P. Goldhammer and E. Feenberg, Phys. Rev. 101, 1233 (1956).

(10) R.A. Cowley and A. D.B. Woods, Can. J. Phys. 49, 177 (1971).

next trial, i. e.,

$$\epsilon^{i+1}(k) = [\epsilon^i(k) + \epsilon^{i+1}(k)]/2. \quad (21)$$

The iterations under this consideration show convergence rapidly in a stable fashion.

In evaluating Eq. (12), $S(k)$ obtained by CF using the HNC and the PY approximations and by Pokrant have been used. Part of results are presented in Tables 1-3 and in Fig. 5. It shows that the HNC data provide the best available in evaluating the excitation spectrum, even though both the PY and Pokrant's data are good in evaluating the the ground-state energy. The small departure from Ref. 1 may be due to numerical error in calculating the single-ring correction energy. By the way, the overshooting of the PY data in Fig. 5 may be attributed to the large first maximum in $S(k)$.

Since $S(k)$ in the HNC approximation yield the best available excitation spectrum, we go on using it to calculate Eq. (13). Results are shown in Table 4 and in Fig. 6. It is seen that contribution from the additional diagrams shown in Fig. 2 are really small except in small k region. This confirms the proper assertion made in Ref. 1, that the neglected two-ring diagrams offer negligibly to the roton minimum but suppress slightly the first peak of the excitation spectrum. Therefore, it seems acceptable to neglect diagrams with two small vertices in the present analysis. The minimum roton energy of this computation is 10.32°K at $k = 1.99\text{\AA}^{-1}$ instead of 8.7°K at 1.9\AA^{-1} by experiment⁽¹⁰⁾. The discrepancy opens to further corrections. Nevertheless, the present consideration by including the two-ring diadiagrams improves the theoretical calculation quite a great deal. The agreement is better than any other theoretical evaluation up to date. However, results show that

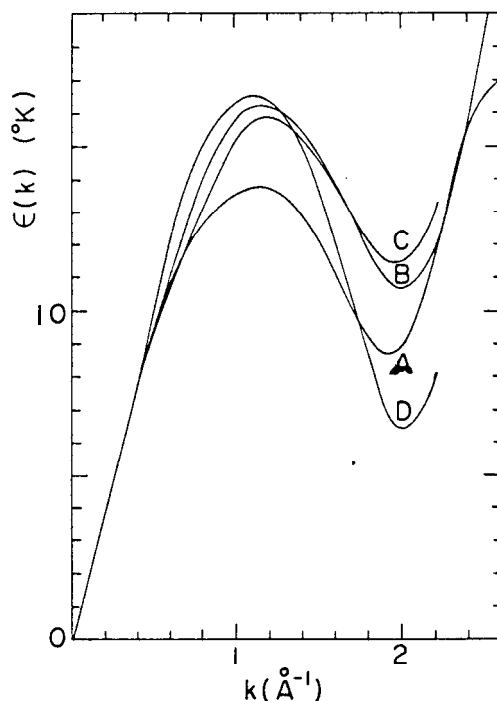


Fig. 5. Theoretical and experimental results for the energy spectrum of elementary excitations. Calculations are done in the optimum BDJ space. Curve A represents the experimental values obtained by Cowley and Woods (Ref. 10). Curves B and D are evaluated making use of $S(k)$ obtained by Campbell and Feenberg (Ref. 2) in the HNC and the PY approximations, respectively. Curve C is evaluated by using $S(k)$ obtained by Pokrant (Ref. 3) with bridge diagrams.

Table 1. Numerical values of Eq. (12), using $S(k)$ obtained by Pokrant³. Wave vectors and energies are expressed in units of \AA^{-1} and $^{\circ}\text{K}$, respectively

k	ϵ_0	ϵ_{2ab}^c	$\Delta\epsilon_{2ab}$	ϵ_{2c}	ϵ_{3ab}	ϵ_{3c}	ϵ_{4a}	ϵ_{4b}	ϵ	error (%)
0.65	12.95	-1.11	-0.04	-0.51	-0.01	-0.19	-0.19	-0.05	10.84	0.45
0.79	15.69	-1.69	-0.05	-0.54	0.01	-0.35	-0.35	-0.11	10.74	0.55
0.85	17.31	-2.12	-0.05	-0.56	0.01	-0.46	-0.46	-0.17	13.77	0.93
0.98	19.44	-2.78	-0.07	-0.58	-0.01	-0.60	-0.60	-0.25	15.00	0.20
1.10	20.99	-3.40	-0.11	-0.61	-0.06	-0.74	-0.74	-0.32	15.70	0.50
1.22	21.93	-3.91	-0.13	-0.63	-0.13	-0.87	-0.87	-0.37	15.90	0.94
1.34	22.20	-4.30	-0.15	-0.68	-0.20	-0.96	-0.96	-0.41	15.56	0.42
1.46	21.02	-4.56	-0.14	-0.74	-0.23	-0.97	-0.97	-0.43	14.92	0.65
1.59	21.24	-4.76	-0.11	-0.84	-0.22	-0.91	-0.91	-0.44	14.00	0.96
1.71	20.37	-4.98	-0.08	-0.97	-0.19	-0.82	-0.82	-0.44	12.91	0.53
1.83	19.70	-5.27	-0.03	-1.13	-0.17	-0.74	-0.74	-0.44	11.90	0.72
1.91	19.59	-5.52	-0.02	-1.24	-0.18	-0.73	-0.73	-0.45	11.46	0.84
1.95	19.71	-5.66	0.04	-1.29	-0.19	-0.73	-0.73	-0.46	11.37	0.86
1.99	19.96	-5.81	0.07	-1.33	-0.20	-0.75	-0.75	-0.47	11.39	0.86
2.03	20.34	-5.97	0.10	-1.37	-0.22	-0.79	-0.79	-0.49	11.51	0.86
2.07	20.86	-6.14	0.14	-1.40	-0.24	-0.84	-0.84	-0.51	11.74	0.83
2.11	21.53	-6.32	0.18	-1.43	-0.26	-0.91	-0.91	-0.55	12.10	0.76
2.16	22.34	-6.50	0.23	-1.45	-0.27	-1.00	-1.00	-0.59	12.56	0.65

Table 2. Numerical values of Eq. (12), using $S(k)$ obtained by Campbell and Feenberg² in the PY approximation

k	ϵ_0	ϵ_{2ab}^c	$\Delta\epsilon_{2ab}$	ϵ_{2c}	ϵ_{3ab}	ϵ_{3c}	ϵ_{4a}	ϵ_{4b}	ϵ	error (%)
0.65	17.07	-1.87	0.02	-0.82	-0.20	-0.44	-0.55	-0.14	13.07	0.47
0.79	20.06	-2.72	0.05	-0.87	-0.17	-0.49	-0.90	-0.29	14.66	0.68
0.85	21.78	-3.31	0.07	-0.91	-0.16	-0.49	-1.15	-0.41	15.41	0.50
0.98	23.85	-4.14	0.09	-0.97	-0.19	-0.41	-1.46	-0.57	16.20	0.99
1.10	25.15	-4.83	0.10	-1.03	-0.26	-0.28	-1.66	-0.66	16.53	0.75
1.22	25.58	-5.30	0.10	-1.11	-0.36	-0.17	-1.72	-0.68	16.34	0.57
1.34	25.10	-5.51	0.09	-1.23	-0.45	-0.15	-1.67	-0.66	15.53	0.31
1.46	23.81	-5.55	0.09	-1.41	-0.49	-0.10	-1.54	-0.63	14.18	0.43
1.59	21.99	-5.53	0.10	-1.67	-0.51	-0.07	-1.36	-0.60	12.35	0.81
1.71	20.05	-5.61	0.13	-2.02	-0.51	-0.05	-1.21	-0.58	10.20	0.72
1.83	18.55	-5.90	0.18	-2.46	-0.55	-0.04	-1.15	-0.59	8.03	0.53
1.91	18.15	-6.22	0.23	-2.76	-0.62	-0.04	-1.18	-0.61	6.94	0.70
1.95	18.18	-6.42	0.27	-2.86	-0.68	-0.04	-1.22	-0.62	6.62	0.73
1.99	18.40	-6.62	0.31	-2.95	-0.74	-0.03	-1.27	-0.64	6.46	0.73
2.03	18.79	-6.83	0.36	-3.02	-0.80	0.00	-1.35	-0.66	6.50	0.67
2.07	19.37	-7.04	0.41	-3.07	-0.87	0.02	-1.44	-0.68	6.69	0.58
2.11	20.12	-7.27	0.46	-3.10	-0.94	0.03	-1.55	-0.71	7.06	0.47
2.16	21.05	-7.49	0.52	-3.12	-1.00	0.04	-1.68	-0.75	7.57	0.36

Table 3. Numerical values of Eq. (12), using $S(k)$ obtained by Campbell and Feenberg² in the HNC approximation

k	ϵ_0	ϵ_{2ab}^c	$\Delta\epsilon_{2ab}$	ϵ_{2c}	ϵ_{3ab}	ϵ_{3c}	ϵ_{4a}	ϵ_{4b}	ϵ	error (%)
0.65	14.22	-1.26	-0.03	-0.56	-0.02	-0.26	-0.24	-0.06	11.79	0.58
0.79	16.95	-1.90	-0.02	-0.60	0.01	-0.30	-0.41	-0.14	13.59	0.60
0.85	18.55	-2.36	-0.02	-0.62	0.02	-0.30	-0.54	-0.21	14.52	0.60
0.98	20.57	-3.07	-0.03	-0.66	0.01	-0.25	-0.72	-0.30	15.54	0.58
1.10	22.00	-3.72	-0.06	-0.69	-0.06	-0.15	-0.87	-0.37	16.07	0.56
1.22	22.80	-4.25	-0.09	-0.73	-0.15	-0.06	-0.99	-0.42	16.12	0.55
1.34	22.96	-4.62	-0.10	-0.78	-0.22	-0.00	-1.05	-0.45	15.72	0.56
1.46	22.53	-4.87	-0.10	-0.86	-0.25	0.02	-1.05	-0.47	14.95	0.68
1.59	21.68	-5.05	-0.09	-0.98	-0.24	0.02	-0.98	-0.47	13.89	0.84
1.71	20.64	-5.26	-0.06	-1.14	-0.21	0.01	-0.88	-0.47	12.62	0.41
1.83	19.77	-5.56	-0.01	-1.33	-0.19	-0.01	-0.80	-0.47	11.39	0.47
1.91	19.56	-5.82	0.04	-1.46	-0.21	-0.03	-0.78	-0.48	10.81	0.51
1.95	19.62	-5.98	0.07	-1.52	-0.22	-0.04	-0.79	-0.49	10.65	0.50
1.99	19.81	-6.14	0.10	-1.57	-0.24	-0.06	-0.82	-0.50	10.58	0.47
2.03	20.14	-6.31	0.13	-1.62	-0.26	-0.07	-0.86	-0.52	10.63	0.46
2.07	20.61	-6.49	0.18	-1.66	-0.29	-0.09	-0.91	-0.54	10.79	0.42
2.11	21.24	-6.68	0.22	-1.69	-0.31	-0.12	-0.99	-0.58	11.09	0.37
2.16	22.02	-6.88	0.28	-1.72	-0.33	-0.15	-1.08	-0.62	11.51	0.32

Table 4. Numerical values of the perturbation energy corrections, using $S(k)$ obtained by Campbell and Feenberg in the HNC approximation

k	ϵ_0	ϵ_{2ab}^c	$\Delta\epsilon_{2ab}$	ϵ_{2c}	ϵ_{4ab}	ϵ_{3c}	ϵ_{4a}	ϵ_{4b}	ϵ_{4c}	ϵ_{4d}	ϵ_{4e}	ϵ	error (%)
0.65	14.22	-1.25	-0.03	-0.56	-0.02	-0.25	-0.23	-0.06	-0.07	-0.10	-0.26	11.39	0.77
0.73	16.08	-1.65	-0.03	-0.58	0.00	-0.29	-0.36	-0.11	-0.10	-0.13	-0.33	12.53	0.70
0.85	18.55	-2.33	-0.02	-0.62	0.02	-0.29	-0.51	-0.20	-0.14	-0.18	-0.43	13.86	0.87
0.98	20.57	-3.0	-0.03	-0.65	0.03	-0.24	-0.69	-0.29	-0.17	-0.21	-0.50	14.78	0.85
1.10	22.00	-3.65	-0.06	-0.68	-0.06	-0.14	-0.83	-0.35	-0.18	-0.23	-0.53	15.29	0.77
1.22	22.80	-4.17	0.08	-0.72	-0.14	-0.06	-0.94	-0.40	-0.17	-0.21	-0.51	15.38	0.67
1.34	22.96	-4.5	-0.10	-0.78	-0.21	-0.00	-1.01	-0.43	-0.15	-0.19	-0.46	15.08	0.58
1.46	22.53	-4.8	-0.10	-0.86	-0.24	0.02	-1.01	-0.46	-0.13	-0.15	-0.39	14.39	0.54
1.59	21.67	-5.01	-0.09	-0.98	-0.24	0.02	-0.95	-0.46	-0.11	-0.12	-0.32	13.42	0.51
1.71	20.64	-5.2	-0.06	-1.14	-0.21	0.01	-0.86	-0.46	-0.09	-0.10	-0.26	12.25	0.48
1.83	19.77	-5.5	-0.01	-1.33	-0.19	-0.01	-0.78	-0.47	-0.07	-0.09	-0.20	11.09	0.45
1.91	19.56	-5.80	0.04	-1.46	-0.20	-0.03	-0.77	-0.47	-0.06	-0.09	-0.18	10.53	0.44
1.95	19.62	-5.95	0.07	-1.52	-0.22	-0.04	-0.78	-0.48	-0.05	-0.09	-0.18	10.38	0.44
1.99	19.81	-6.11	0.10	-1.57	-0.24	-0.06	-0.81	-0.50	-0.05	-0.09	-0.17	10.32	0.42
2.03	20.14	-6.28	0.13	-1.62	-0.26	-0.07	-0.85	-0.51	-0.05	-0.09	-0.17	10.37	0.40
2.07	20.61	-6.46	0.18	-1.66	-0.28	-0.09	-0.90	-0.54	-0.04	-0.10	-0.18	10.54	0.37
2.11	21.23	-6.65	0.22	-1.69	-0.34	-0.12	-0.98	-0.57	-0.04	-0.10	-0.18	10.83	0.35
2.20	22.96	-7.03	0.33	-1.74	-0.34	-0.19	-1.18	-0.66	-0.04	-0.11	-0.19	11.81	0.51
2.32	26.59	-7.77	0.56	-1.78	-0.31	-0.40	-1.66	-0.90	-0.05	-0.12	-0.22	13.93	0.58
2.44	31.14	-8.67	0.85	-1.79	-0.15	-0.77	-2.26	-1.22	-0.07	-0.14	-0.25	16.69	0.54

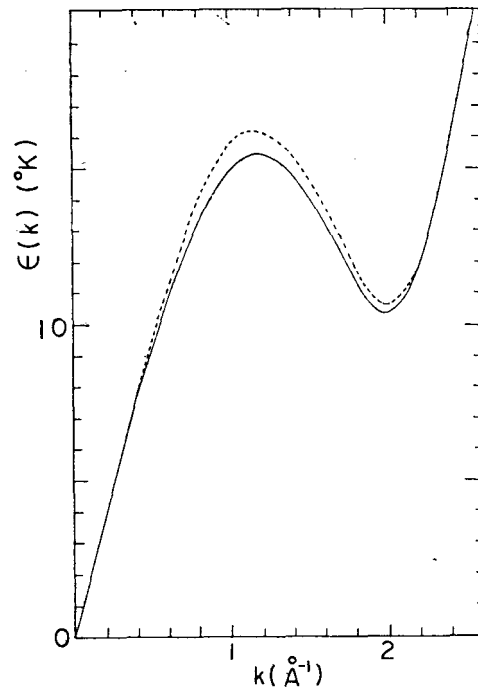


Fig. 6. Theoretical calculations for the elementary excitation in the BDJ method. Evaluations are done with $S(k)$ obtained by CF in the HNC approximation: dashed curve for Eq. (12) and solid curve for Eq. (13).

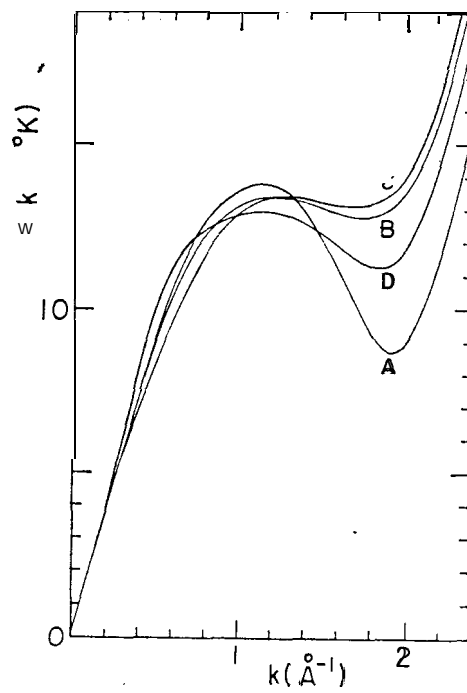


Fig. 7. Theoretical and experimental results for the elementary excitation energy. Calculations are finished by using the Jackson and Feenberg⁵ method. Different curves represent the same use of $S(k)$ described in Fig. 5.

the present analysis breaks down completely over region $k \leq 2.56 \text{ \AA}^{-1}$, where stable plateaus may occur instead of quadratic increasing.

As for the JF method, one encounters with the need of the exact $\mathbf{S}(\mathbf{k})$. As mentioned before, this $\mathbf{S}(\mathbf{k})$ is difficult to obtain accurately even if possible. So far approximate data from the X-ray scattering and the HNC have been used⁽⁵⁻⁸⁾ extensively. If the optimum $\mathbf{S}(\mathbf{k})$ may be used to apply Eq. (20), we give rise to results shown in Fig. 7. The excitation spectrum shows so disappointed that the roton minimum is not obvious and stays slightly high in comparison with experiments. For example, in the use of $\mathbf{S}(\mathbf{k})$ under the PY approximation, the minimum roton energy is 11.26°K at $K = 1.83 \text{ \AA}^{-1}$. The difficulty primarily comes from the term $\epsilon_3(k)$, which appear in general positive and comparable to other two-ring diagrams. Hence the inclusion of ϵ_3 strongly cancels the correction generated by the single-ring perturbation. The anomalous effect of ϵ_3 may be explained as due to the improper use of the optimum $\mathbf{S}(\mathbf{k})$ as exact.

V. CONCLUSION

The optimum BDJ method including the two-ring energy corrections can generate excitation spectrum in good agreement with experiment. In the present analysis, it shows that further consideration of higher -order corrections seem hardly affecting the minimum roton energy. In order to have improved theoretical calculations, the accurate $\mathbf{S}(\mathbf{k})$ and the proper expression of $P^{(3)}$ are unavoidable. Alternatively, the JF method provides an easier way with less perturbation diagrams than the optimum BDJ in representing the elementary excitation energy. However, the inconvenient exact $\mathbf{S}(\mathbf{k})$ is required. If one can solve the Hamiltonian (2), and carry out the exact $\mathbf{S}(\mathbf{k})$ accurately, then, the JF method should yield the best and the easiest way to the excitation spectrum. Anyhow, this problem is still open.